Published by IOP Publishing for Sissa Medialab

Received: *September 11, 2024*
Revised: *November 8, 2024*
Accepted: *December 3, 2024*
Published: *December 23, 2024*

TECHNICAL REPORT

Development of a sub-mm particle tracking detector based on a plastic scintillator with SiPM charge sharing

R. Gargiulo[a,*] **Vittoria Ciccarella**[a] **Elisa Di Meco**[b] **Eleonora Diociaiuti**[b] **and Ivano Sarra**[b]

[a] *Sapienza University of Rome, Piazzale Aldo Moro 5, Rome, Italy*
[b] *INFN National Frascati Laboratories, Via Enrico Fermi 54, Frascati, Italy*

E-mail: ruben.gargiulo@uniroma1.it

Abstract: This paper presents the development and performance of the particle tracker employing a $3 \times 3\,\mathrm{cm}^2$ plastic scintillator tile with sixteen $4 \times 4\,\mathrm{mm}^2$ SiPMs coupled to one of its faces. The light distribution inside the scintillator allows to reconstruct the hit position using charge information of all the SiPMs. Performance tests were conducted at the Frascati National Laboratory Beam Test Facility (LNF-BTF) using a 450 MeV electron beam. The device showed MIP-counting capabilities, high efficiency (96%), good timing (170 ps) and sub-mm resolution in the x-y coordinates.

Keywords: Particle tracking detectors; Scintillators, scintillation and light emission processes (solid, gas and liquid scintillators); Trigger detectors; Timing detectors

*Corresponding author.

https://doi.org/10.1088/1748-0221/19/12/T12006

2024 JINST 19 T12006

Contents

2024 JINST 19 T12006

1 Introduction

Plastic scintillators detectors play a crucial role in high-energy physics experiments, due to their low cost, high availability and light output and good timing properties. Moreover, coupling silicon photo-multipliers (SiPM) to scintillators represents a very effective solution due to their low cost, very fast timing and good resolution on photo-electron number.

The following pages will focus on the development and performance of a particle tracking device employing a $3 \times 3\,\mathrm{cm}^2$ plastic scintillator tile with sixteen uniformly distributed SiPMs coupled to one of its faces with optical glue. The light distribution inside the scintillator allows reconstructing the hit position using charge information of all the SiPMs, i.e., evaluating positions with averages of SiPMs center coordinates, weighted with SiPMs charges. A beam test was conducted at the Frascati National Laboratory Beam Test Facility (LNF-BTF) using a 450 MeV single-particle electron beam. The device showed capability to count particles event-by-event while ensuring high efficiency (96%), good timing (170 ps) and sub-mm resolution in two coordinates.

The detector described represents an effective and low-cost solution for experiments or beam tests requiring to detect and count charged particles with good efficiency, timing and tracking performances, for example to reject the presence of neutral particles or multiple charged particles when a sub-mm resolution is sufficient. SiPMs signals can be acquired with standard commercial flash-ADCs, allowing very easy synchronization with other detectors, for example in small experiments and beam tests.

Silicon detectors provide a solution for this type of purposes, allowing outstanding tracking resolutions of the order of microns, but show worse timing properties in general and have much higher cost and complexity, making it difficult to synchronize their acquisition with detectors of other types.

Moreover, other detectors design providing sub-mm position resolution with plastic scintillators employ very different readout technique like CMOS cameras [1, 2], which have the same disadvantages as silicon detectors. It should be also pointed out that, because of different design choices, other systems similar from the technological point of view to the one showed in this paper, i.e., featuring scintillators and SiPMs, do not reach sub-mm resolution [3].

2 Detector design

The detector uses Eljen Technology EJ-200 plastic scintillator tiles, each measuring $3 \times 3\,\mathrm{cm}^2$, to exploit EJ-200 high light output of approximately 10^4 photons per MeV, fast rise time of 0.9 ns, and decay time of 2.1 ns. The light from the scintillator is detected by 16 Hamamatsu S14160-4050HS SiPMs, each operated at a voltage of 41V and covering an area of $4 \times 4\,\mathrm{mm}^2$, resulting in a SiPM/scintillator area ratio of 28%. Each SiPM consists of $50 \times 50\,\mu\mathrm{m}^2$ pixels, providing a photon detection efficiency (PDE) of 52% at a wavelength of 420 nm (matching the spectral peak of EJ-200) and a gain of 2.7×10^6. A 3M™ Enhanced Specular Reflector (ESR) foil matching the scintillator size was placed on the face opposite to SiPMs and coupled with optical grease, in order to improve the light collection. It is possible that the use of a diffusive or a black foil instead of the ESR could improve the position resolution, but it would have spoiled the light collection efficiency, thus worsening detection efficiency, timing and particle counting capabilities.

The SiPMs are coupled to the scintillator tile using optical glue, ensuring a stable and efficient optical connection and are than wire-connected to an electronic front-end customized for SiPM readout [4]. The entire assembly is housed in a 3D printed box to maintain alignment and stability, as showed in figure 1.

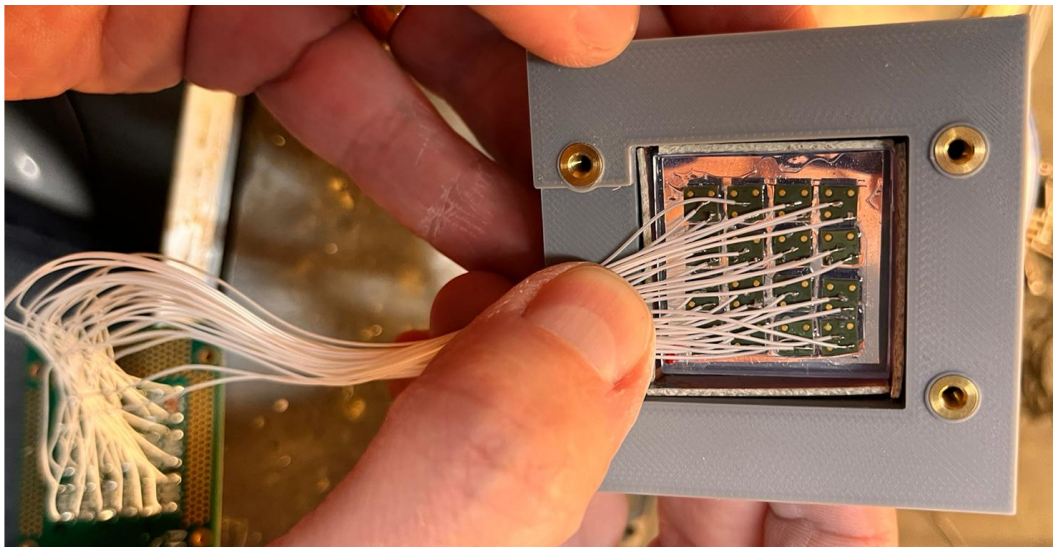

Figure 1. Picture showing the 3D printed box with scintillator and SiPMs, along with the wires connecting the SiPMs to the front-end board.

SiPMs signals are processed by an analog circuit providing shaping and a factor of 10 electronic gain and are then digitized by means of a CAEN V1742 with sampling rate set to 5 GS/s and acquisition windows of 1024 samples (204.8 ns).

A ratio of 0.23 p.e./pC between number of photo-electrons and charge is estimated using the 2.7×10^6 SiPM and 10 FEE gains information.

The whole assembly with the detector and the front-end board is mounted on a steel block for stability, as showed in figure 2.

The positions of SiPMs with respect to the scintillator tile edges were measured during assembly, as shown in figure 3, in order to employ them for data analysis.

2024 JINST 19 T12006

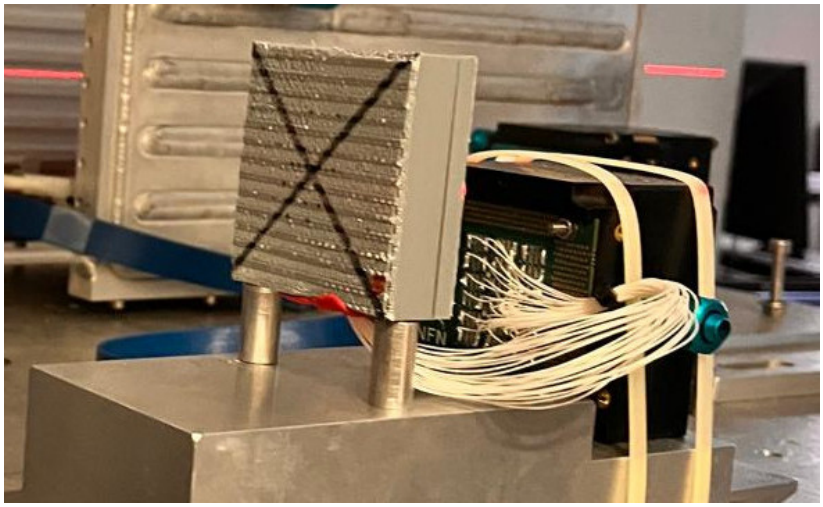

Figure 2. Picture showing the whole detector assembly in LNF-BTF during beam test.

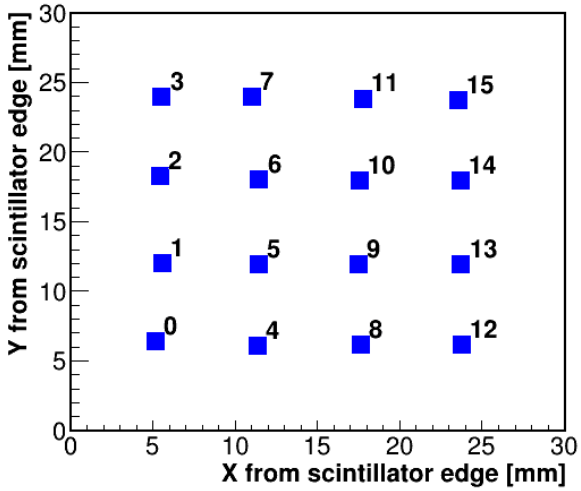

Figure 3. Plot showing the position of each SiPM (labelled with the corresponding channel on the digitizer).

3 Beam test and performances

The performances were evaluated with a beam test at Frascati National Laboratory Beam Test Facility (LNF-BTF) [5] using a 450 MeV single-particle electron beam, hence providing a number of particles around one (with a Poisson distribution) for each bunch (1 every 25 Hz). The detector was placed on an optical 2-axis motorised stage. Alignment was achieved using a laser system at the BTF. During test runs a Fitpix silicon detector is placed upstream in order to monitor the beam spread, showing a 0.4 mm Gaussian spread in x and y, while it is removed during data-taking.

A calorimeter consisting of a spare lead-glass module of the NA62 Large Angle Veto [6] readout by a large area PMT (featuring a $< 10\%$ resolution at the beam energy) was placed downstream and acquired together with the tracking detector in order to absorb and monitor the beam. Data acquisition was triggered per bunch at the BTF rate of 25 Hz, regardless of the delivered number of particles per bunch. A series of beam tests were conducted, each targeting different positions on the scintillator tile,

2024 JINST 19 T12006

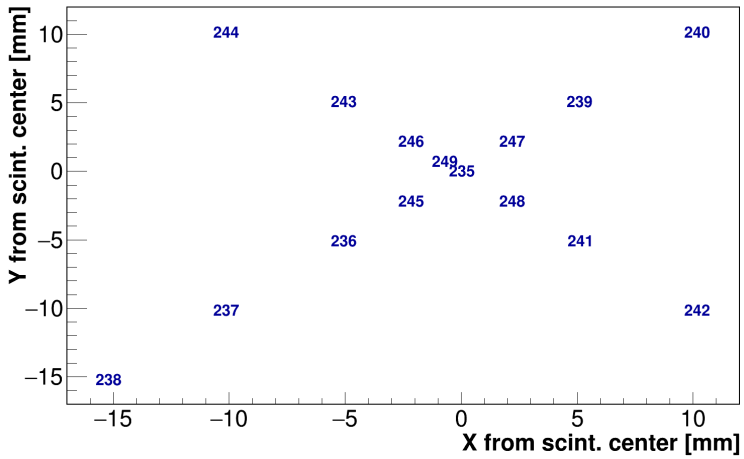

Figure 4. Plot showing the position of the beam center for each run (labelled with a chronological index), with respect to the detector center.

by moving the table hosting the detector. These tests included scans along two diagonals at distances of 2.5, 5, and 10 mm from the center, as well as a run at 1 mm, as shown in figure 4.

Both SiPMs and lead glass charge depositions were measured from the waveform integral, while the timing was evaluated interpolating the waveforms with a cubic spline and finding the time at a threshold corresponding to an 11% constant-fraction of the signal amplitude.

3.1 Total charge spectrum and particle counting

Both total scintillator charge (sum of all SiPM charges) and lead glass charge spectra allow distinguishing between one and two particle events, as shown from the fits in figure 5 and figure 6 for data acquired with beam impinging at the center of the tile (central run). The MIP most probable energy deposit, for

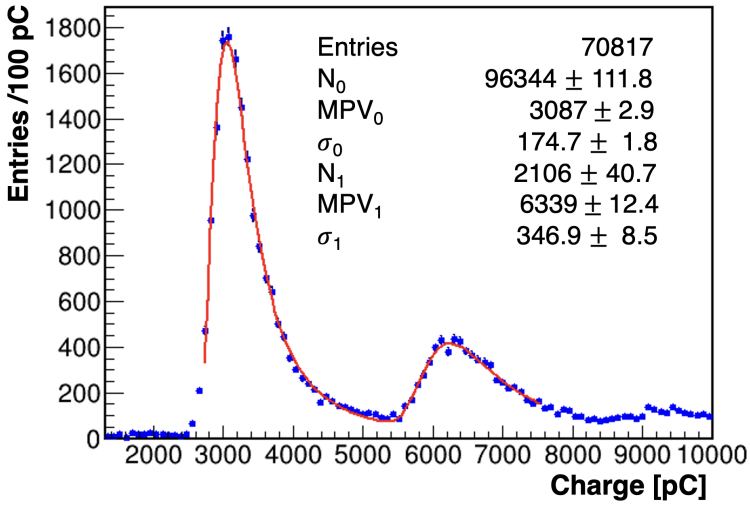

Figure 5. Distribution of total charge on tracking detector, fitted with two Landau functions, as expected for MIP-like deposits corresponding to one and two particles events. The fit parameters corresponds, respectively, to the amplitude, most probable value (MPV) and FWHM/4 (σ) of the two Landau functions.

2024 JINST 19 T12006

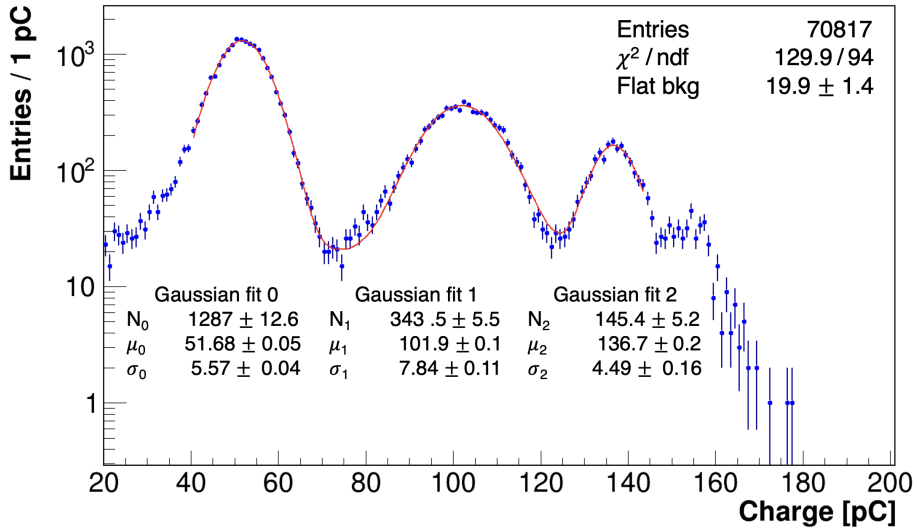

Figure 6. Distribution of lead glass charge, fitted with three Gaussian functions together with a small flat background, as expected for total energy deposits corresponding to one, two and three particles events.

a 0.5 cm thick EJ-200 scintillator, is about 1 MeV, while the number of photo-electrons per MIP is ~ 710, estimated from the 3087 pC peak charge for one-particle events. This light yield is compatible with a $\epsilon_{\text{light}} = 50\%$ light collection efficiency as extrapolated from the following relation:

$$10^4/\text{MeV} \cdot 1\,\text{MeV} \cdot \epsilon_{\text{area}} \cdot \text{P.D.E.} \cdot \epsilon_{\text{light}} \sim 710\,\text{p.e.} \tag{3.1}$$

where 10^4 photons per MeV is the nominal light output for EJ-200, $\epsilon_{\text{area}} = 28\%$ is the total SiPM/scintillator area ratio and P.D.E. = 52% is the SiPM photon detection efficiency.

The noise level of each channel was studied by evaluating its charge RMS in the acquisition window with random triggers, obtaining a value of 3.5 pC, which translates to 14 pC on the total charge on all channels. The impact on the noise can therefore be considered very limited, given the much larger charges collected for signal events.

A simple cut on the total charge can be used to reject events with more than one particle. Efficiencies were evaluated with two cuts (4000 and 5000 pC), by considering the fitted number of events for one and two particle events (from the lead glass charge distributions) before and after the cuts, as shown in figure 7.

An efficiency of 83% (93%) on one particle events and 3% (5%) on two particle events was evaluated after cuts $Q < 4000(5000)$ pC on total charge. These values show very good particle-counting capability for the tested detector. For this data analysis, however, it was preferred to select one particle events in a slightly cleaner way, i.e., employing a stronger cut between 30 and 70 pC on the lead glass charge.

3.2 Position reconstruction

The x and y positions were reconstructed using charge-weighted averages of SiPMs center positions. The resulting distributions were fitted with two Gaussian functions, in order to better catch asymmetries, and to measure per-run yield, mean and resolution, as shown in figure 8. Unfortunately, edge effects,

2024 JINST 19 T12006

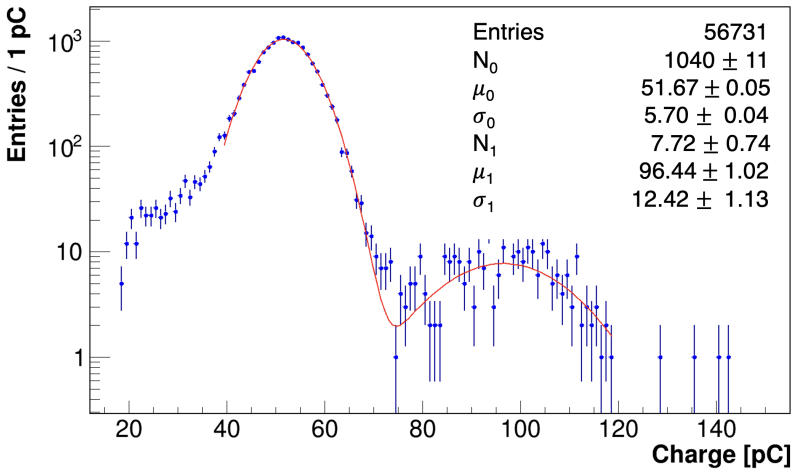

(a) Cut $Q < 4000$ pC on tracking detector total charge.

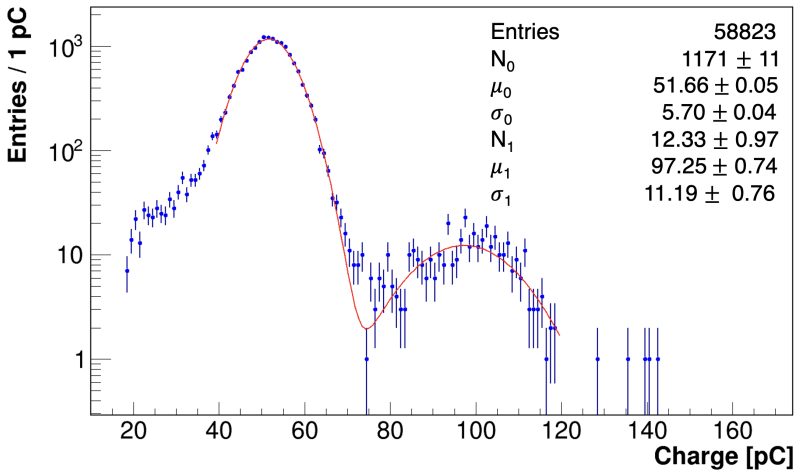

(b) Cut $Q < 5000$ pC on tracking detector total charge.

Figure 7. Distribution of lead glass charge after a cut on total charge on the tracking detector, fitted with two Gaussian functions, as expected for calorimetric deposits corresponding to one and two particles.

with increased asymmetry, are visible at 10 mm from the center, where there are the last SiPMs of the assembly and the light is shared mainly with the scintillator edge.

A fifth-order polynomial function was used to calibrate the position reconstruction, by fitting the true beam positions with respect to the reconstructed mean positions, as shown in figure 9. The calibration curve was employed to propagate uncertainties through derivatives.

The resulting uncertainty, coming from the resolution of the two Gaussian functions fitted for each run, was further corrected, by subtracting in quadrature the contribution from beam energy spread estimated with the Fitpix (0.4 mm), as shown in figure 10.

The resolution of the detector ranges from around 0.7 mm in the central region to around 1.5 mm in the outer region (at 1 cm from the center).

By using resolutions, true and reconstructed coordinates, the normalized residuals were evaluated, and shown in figure 11.

2024 JINST 19 T12006

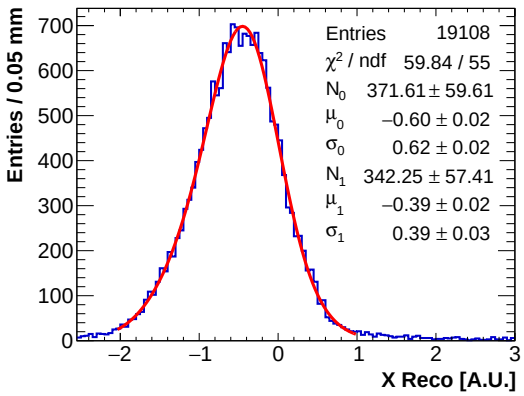

(a) At 0 mm from the center

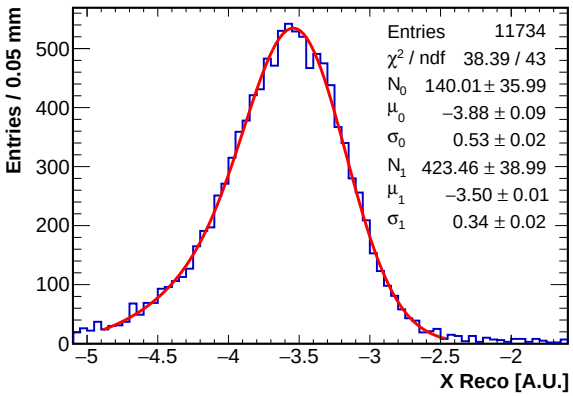

(b) At 5 mm from the center

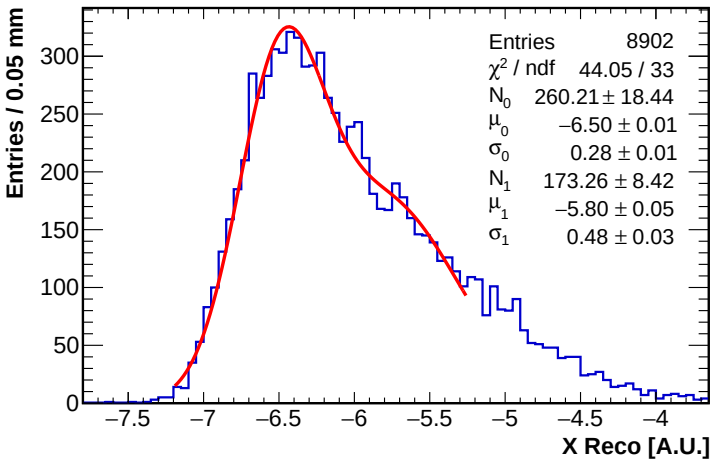

(c) At 10 mm from the center

Figure 8. Distribution of x reconstructed position, evaluated using SiPMs center positions in mm, with the beam at 0, 5, and 10 mm from scintillator center, along a diagonal.

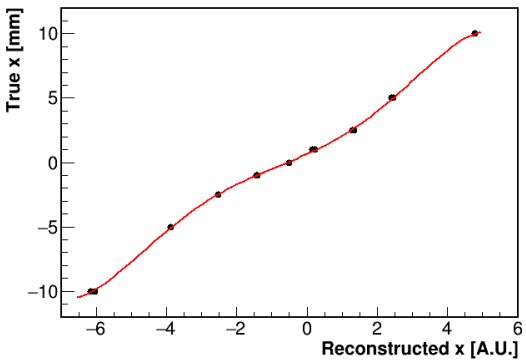

(a) Calibration curve for x.

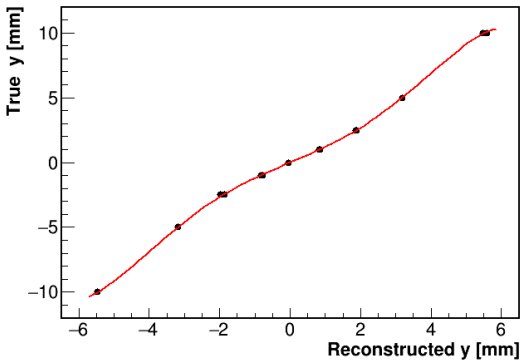

(b) Calibration curve for y.

Figure 9. Calibration curve (5-th order polynomial) between true coordinates and reconstructed coordinates.

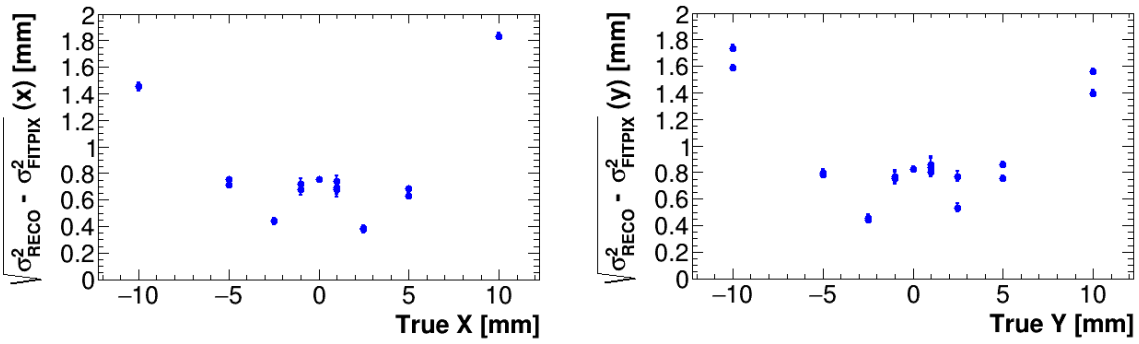

(a) Resolution for x.

(b) Resolution for y.

Figure 10. Position resolution vs. true coordinates.

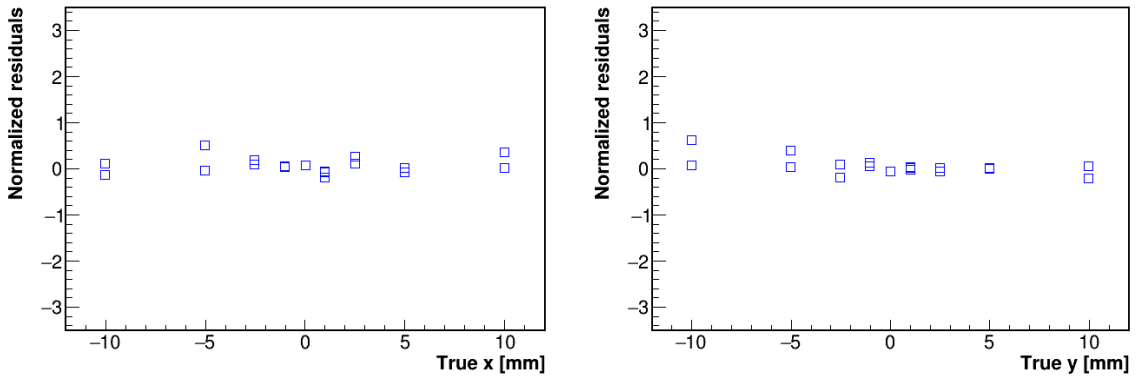

(a) Normalized residuals for x.

(b) Normalized residuals for y.

Figure 11. Normalized residuals after calibration.

The SiPMs are placed at a distance of about 6 mm between each other, therefore, if one considers an envelope of ±3 mm around each SiPM center, they sample uniformly a region of $2.4 \times 2.4\,\mathrm{cm}^2$ in $6 \times 6\,\mathrm{mm}^2$ squares. Without using charge information, the resolution would be 1.7 mm, i.e., the one corresponding to a uniform distribution with a 6 mm spread. Hence, by exploiting charge information, a large and interesting improvement of a factor 2.5 is made in the central region.

The position reconstruction procedure comes naturally with an efficiency to be evaluated. As a first step, for each run, the fitted number of events (from the same two Gaussian functions used to evaluate mean and resolution) was divided by the number of events satisfying the lead glass cuts to select single particle events. Then, a correcting scale factor near 1, found by comparing the cut-and-count (from 30 to 70 pC) number of events, to the one fitted from the lead glass distribution with a function comprising two Gaussians and a flat background, as shown in figure 12.

Very high efficiencies, around 96%, were found for all runs, as shown in figure 13.

3.3 Timing

Timing performances were evaluated using time differences between near channels, i.e., ch9 and ch10 (see figure 8) for the run at the center. A time resolution $\sigma_{\Delta T} \sim 250\,\mathrm{ps}$, corresponding to a single-channel $\sigma_T \sim 170\,\mathrm{ps}$, as shown in figure 14.

2024 JINST 19 T12006

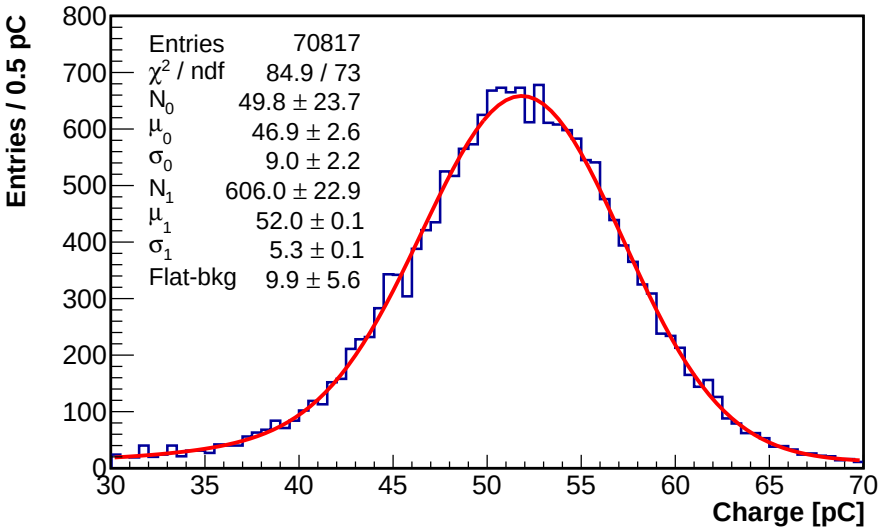

Figure 12. Distribution of lead glass charge for the region used to select one particle events (30 to 70 pC), fitted with two Gaussian functions, together with a flat background.

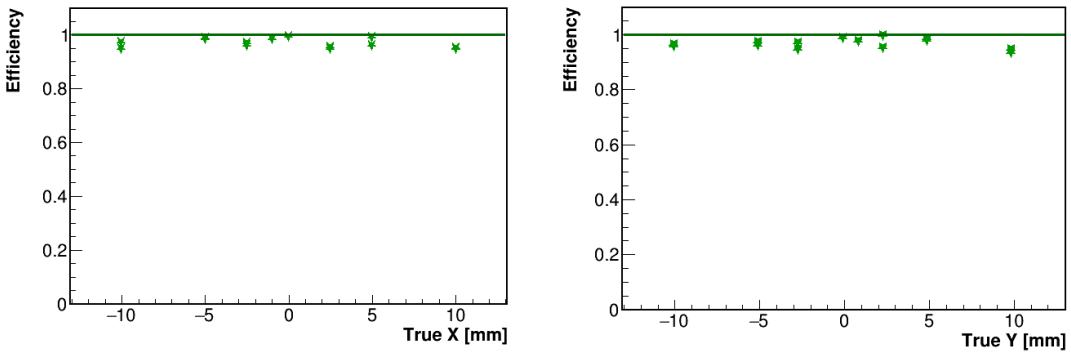

(a) Efficiency vs. x.

(b) Efficiency vs. y.

Figure 13. Efficiency with respect to x and y position.

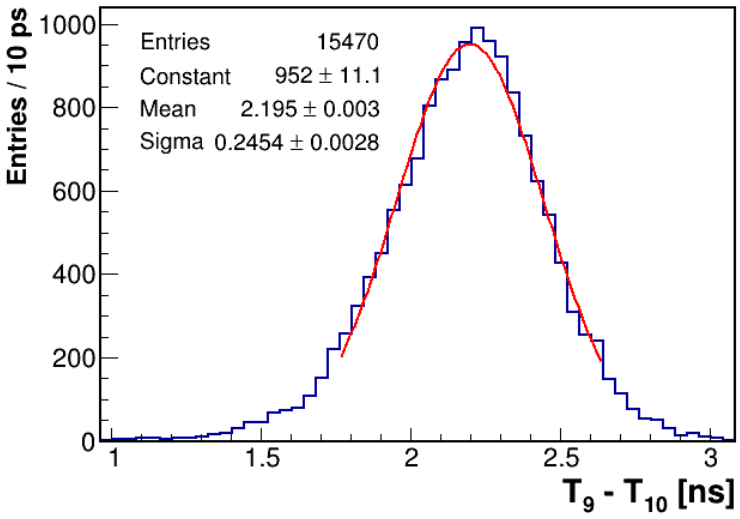

Figure 14. Distribution of time differences between ch9 and ch10, fitted with a Gaussian function.

2024 JINST 19 T12006

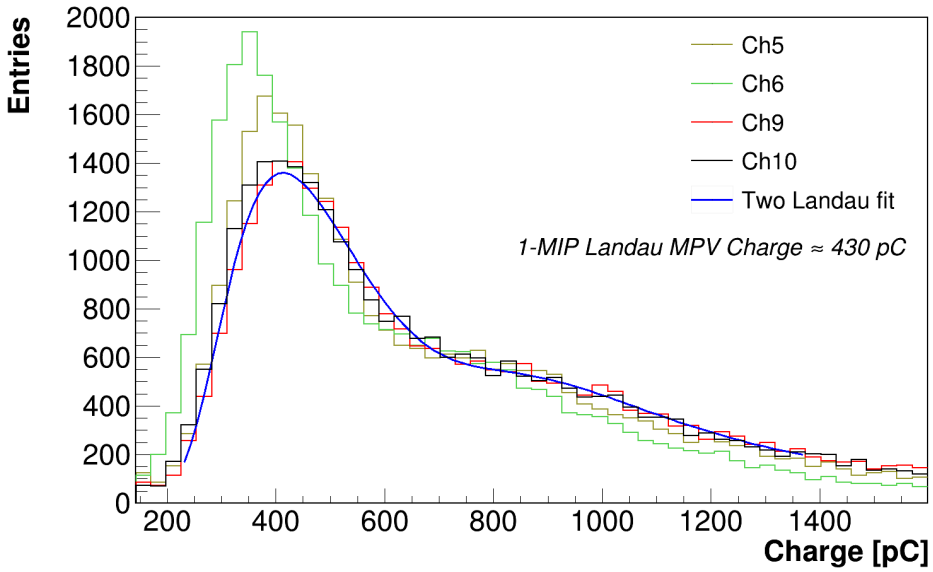

Figure 15. Distribution of charge for channels near detector center, without any cuts, fitted with two Landau functions.

For both channels, the most probable number of photoelectrons for the Landau function corresponding to one particle events is about 100, as shown in figure 15.

The obtained value is close to the ultimate coincidence time resolution [7]:

$$CTR \sim \sqrt{\frac{\tau_r \tau_d}{N_{p.e.}}} \sim 140\,\text{ps} \tag{3.2}$$

where τ_r and τ_d are, respectively, rise and decay times of EJ-200.

4 Conclusions

The development, assembly and test of a particle tracking device based on a $3\times3\,\text{cm}^2$ plastic scintillator tile coupled with sixteen $4\times4\,\text{mm}^2$ SiPMs demonstrated several key performance attributes. A beam test conducted at the Frascati Beam Test Facility (LNF-BTF) using a 450 MeV electron beam revealed effective particle counting capabilities using total charge information. The position reconstruction method, based on charge sharing among the SiPMs, provided sub-mm spatial resolution in both x and y coordinates in its central region, where the edge effects are not relevant. The tracking device achieved high detection efficiency, approximately 96%, for single particle events. The timing performance of the device was good, with a time resolution of about 170 ps per channel.

Overall, the developed tracking device presents a low-cost, efficient solution for applications requiring particle detection and counting with good timing and spatial resolution. The integration of SiPMs with plastic scintillators offers significant advantages in terms of simplicity, synchronization with other detectors, and performance, making it a suitable choice for various experimental setups and beam tests.

Acknowledgments

The authors wish to thank the LNF Division Research departments for their technical and logistic support. They also thank the whole BTF staff for providing the beam time and helping them in getting

2024 JINST 19 T12006

a smooth running period. They express their warmest thanks to L. Foggetta and D. Di Giovenale for adjusting and tuning the beam to the detector needs. Appreciation is also given to A. Russo and L. Salvatori who contributed to the assembly and development phases of this project.

References

[1] M. Clark et al., *Ultra-fast, high spatial resolution single-pulse scintillation imaging of synchrocyclotron pencil beam scanning proton delivery*, *Phys. Med. Biol.* **68** (2023) 045016.

[2] G.Z. Woźniak and B. Kozłowska, *High resolution 2D plastic scintillator detectors for radiotherapy departments*, *Polish J. Med. Phys. Eng.* **29** (2023) 92.

[3] Y. Simhony et al., *Scintillator-SiPM detector for tracking and energy deposition measurements*, *Nucl. Instrum. Meth. A* **1069** (2024) 169955 [arXiv:2406.19652].

[4] S. Ceravolo et al., *Crilin: A CRystal calorImeter with Longitudinal InformatioN for a future Muon Collider*, 2022 *JINST* **17** P09033 [arXiv:2206.05838].

[5] B. Buonomo, C. Di Giulio, L.G. Foggetta and P. Valente, *The Frascati LINAC Beam-Test Facility (BTF) Performance and Upgrades*, in the proceedings of the *5th International Beam Instrumentation Conference*, Barcelona, Spain, September 11–15 (2016) [DOI:10.18429/JACoW-IBIC2016-TUPG29].

[6] F. Ambrosino et al., *The Large Angle Photon Veto System for the NA62 Experiment at CERN*, *Phys. Procedia* **37** (2012) 293.

[7] S. Gundacker, R.M. Turtos, E. Auffray and P. Lecoq, *Precise rise and decay time measurements of inorganic scintillators by means of X-ray and 511 keV excitation*, *Nucl. Instrum. Meth. A* **891** (2018) 42.

2024 JINST 19 T12006